MDPI

Article

Study on the Catalytic Oxidation Modification Effect of Heavy Oil at Low Temperature under the Action of Different Ligand Ferric-Based Systems

Dichen Tan, Zhaofei Ma *, Lian Chen, Yuanzhu Mi [ID] and Xuemin Yan *[ID]

College of Chemistry and Environmental Engineering, Yangtze University, Jingzhou 434023, China;
18163309329@163.com (D.T.); 18171715690@126.com (L.C.); michem@yangtzeu.edu.cn (Y.M.)
* Correspondence: libramzf@126.com (Z.M.); xueminyan@126.com (X.Y.)

Abstract: This work explores the low-temperature catalytic oxidation of heavy oil (140 °C), resulting in structural changes with reduced heavy components and increased light components. The catalytic oxidation system consists of a catalyst, an oxidant, and a proton donor. Four different complexes of iron-based catalysts were utilized: ferric oleate, iron naphthenate, EDTA–FeNa, and EDDHA–FeNa. Catalytic oxidation processes with these catalysts produced four types of oxygenated oil, which were then analyzed using group composition analysis and a viscosity test. The results show that EDDHA–FeNa is more favorable for the catalytic oxidation of heavy oil in a low-temperature environment, achieving a viscosity reduction rate of 78.57%. Furthermore, the catalytic performance of heavy oil oxidation was investigated using EDDHA–FeNa as catalyst under three conditions: the amount of catalyst, oxidant and reaction temperature. These findings may provide researchers valuable guidance and principles for the investigation and development of advanced catalytic viscosity reduction of heavy oil.

Keywords: heavy oil; catalyst; low temperature; catalytic oxidation

1. Introduction

Heavy oil can be upgraded catalytically via aquathermolysis viscosity reduction and catalytic oxidation technologies. Using them may result in an irreversible drop in the viscosity of heavy oils [1–3]. Injecting a cracking catalyst into a heavy oil reservoir at high temperatures (>200 °C) decreases the apparent viscosity of the heavy oil [4,5]. In contrast, catalytic oxidation reactions occur at low temperatures, often below 160 °C. Catalytic oxidation technology integrates various types of oil recovery methods, such as oxidation modification and self-emulsification. In terms of the mechanism, the essence of low-temperature catalytic oxidation technology lies in the removal of heteroatoms, which is demonstrated by effectively breaking the heteroatom side chain of polycyclic aromatic hydrocarbon and weakening the hydrogen bond between the lamellar structures of heavy oil [6]. This can effectively increase the viscosity reduction rate of heavy oil, improving the quality of crude oil and enhancing the flowability of heavy oil. The technology has the advantages of low cost, low temperature, mild reaction conditions, and easy operation, effectively promoting the recovery of heavy oil. The key to low-temperature catalytic oxidation technology is the preparation of special catalysts to improve the efficiency of the low-temperature oxidation reaction of heavy oil, as well as the oxidation of C-R (R = S, N, O) bonds into alcohols, aldehydes, or carboxylic acids, which are located on the side chains of polycyclic aromatic hydrocarbon of heavy oil [7–9].

Among the catalysts that can be used for the catalytic oxidation of heavy oil, transition metal-based catalysts are particularly prominent, especially ferric-based catalysts. The outer valence electron configuration of the iron element is $3d^6 4s^2$; when the outermost electrons are lost, an empty orbit is created, and the ferric ion is obtained, which is electrophilic. If

a heteroatom containing lone pair electrons is nearby, the ferric ion nucleus will attract the lone pair electrons, which will rapidly fill the hole. Thus, the metal active center of the catalyst attacks the C-R (R = S, N, O) bonds, and the reactive oxygen seals the end forming oxygen-containing groups. Catalysts such as ferric oleate, iron naphthenate, ferric dodecylbenzene sulfonate, ferric acety-lacetonate, metallic oxide nanoparticles, and so on, have been used in aquathermolysis and the catalytic oxidation of heavy oil, showing better modification effects and better viscosity reduction [10–17]. Zhou [18] compared γ-Al$_2$O$_3$ and Fe$_3$O$_4$ nanoparticles with a traditional displacement agent for heavy oil upgrading. They found that Fe$_3$O$_4$ nanoparticles can promote the upgrading of heavy oil, improving the oxygen consumption rate of heavy oil catalytic oxidation at low temperatures. Li [19] found that α-Fe$_2$O$_3$ has a strong effect on asphaltene modification, reflected in the reduction of S and N content, the reduction of aromatic degree, and the reduction of viscosity from 161,180 mPa·s to 45,882 mPa·s.

However, although nanoparticle catalysts exhibit good catalytic modification performance, their application is limited due to their characteristics of easy agglomeration and problematic injection formation. Therefore, the catalytic performance of the ferric-based organic complex needs to be further studied because they easily come into contact with oil and can be easily injected into the formation.

In addition, an oxidant plays an indispensable role in the process of heavy oil modification. Previously, researchers have conducted a series of catalytic oxidation studies using air as an oxidizing agent in the process. However, if the petroleum reservoir is fractured or a cavity reservoir, the injected air will have insufficient contact with the heavy oil, reducing the efficiency of the reaction. At the same time, gas is prone to leak out. If a large amount of air is concentrated in the producing well, and the oxygen content exceeds the safety threshold (5%), the well becomes highly susceptible to explosion [9].

Based on this, hydrogen peroxide has gradually gained attention as a highly efficient oxidant, but it is easily decomposed and has poor stability, which poses safety risks and limits its application conditions. Therefore, there is a need to switch to other relatively safer oxidants, such as organic peroxides, most of which are more stable than inorganic peroxides. Previous research has shown that tert-butyl hydroperoxide can make complete contact with heavy oil and boost the upgrading effect under the action of a catalyst.

Our research group has previously synthesized Ni-based and Fe-based catalysts, which have demonstrated superior catalytic modification properties for heavy oil [20,21]. In order to explore the catalytic effect of ferric-based organic complex, four kinds of ferric-based catalysts have been selected to investigate the catalytic oxidation performance of heavy oil from the Tahe oilfield in Xinjiang, with the reaction temperature ranging from 100 °C to 180 °C. This study provides a theoretical framework for improving heavy oil recovery and lowering viscosity at low temperatures.

2. Results and Discussion

2.1. Viscosity Reduction Process of Heavy Oil

2.1.1. Effect of Catalyst Type on Experimental Results

As shown in Figures 1 and 2, when compared with crude oil, the asphaltene content of the oxidized oil obtained by the four catalysts decreases, while the viscosity reduction rate of the oxidized oil increases. The content of asphaltenes after the reaction of ferric oleate and iron naphthenate is reduced by 1.7% and 0.81%, respectively, and the viscosity reduction rates are 75.38% and 75.59%. The content of asphaltenes after the reaction of EDTA–FeNa and EDDHA–Fe has decreased by 2.57% and 3.97%, respectively, and the viscosity reduction rate of both exceeds 80%. Among the four catalysts, EDDHA–Fe has the highest degree of asphaltene reduction and viscosity reduction rate. Although ferric oleate and iron naphthenate are common oil-soluble organic ligands, the generated metal complexes are easier to come into contact with oil products, but the effect is not better than that of EDTA–FeNa and EDDHA–FeNa in terms of group composition and viscosity reduction rate. The metal center of the catalyst, ferric ion, has a vacant orbit and is

electrophilic. Although under ordinary conditions, EDDHA–FeNa is hexacoordinate with no available coordination site, dissociation of one or more of the donor atoms of the ligand may well happen at elevated temperatures, providing an opportunity for coordination of S and N-containing components of the oil to the Fe(III) center. Therefore, EDDHA–FeNa is a suitable catalyst for the catalytic oxidation of heavy oil.
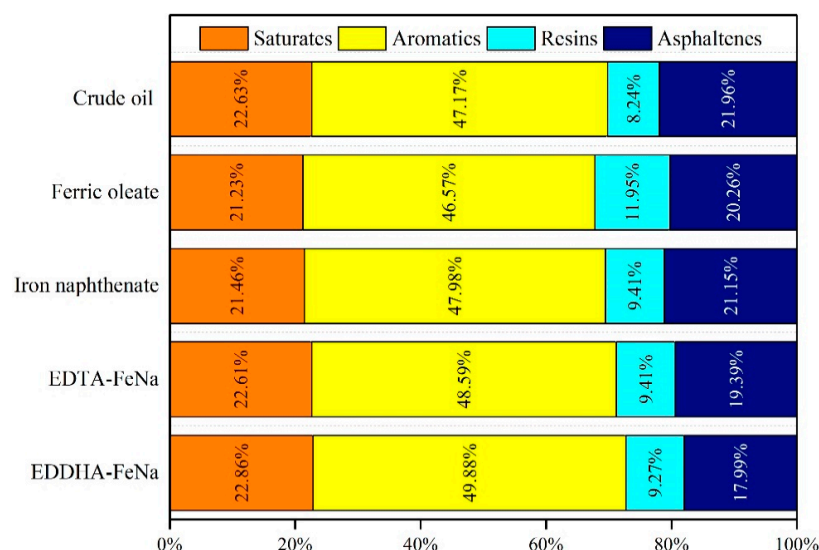

Figure 1. Effect of ferric-based catalysts with different ligands on heavy oil group composition.
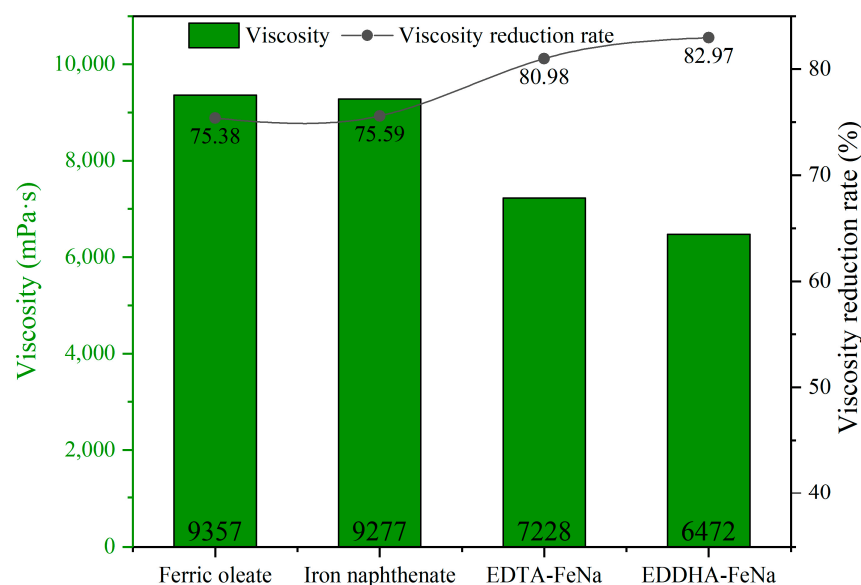

Figure 2. Effect of ferric-based catalysts with different ligands on the viscosity of heavy oil. (The viscosity of oil sample is 38,010 mPa·s at 50 °C).

2.1.2. Effect of Amount of Catalyst

As shown in Figure 3, when no catalyst was used, the heavy components in the heavy oil increased significantly. However, when the catalyst EDDHA–FeNa was added, the heavy components were significantly reduced. In addition, the amount of catalyst also affects the group composition of heavy oil. When the catalyst concentration ranges from 0.05% to 0.1%, the heavy components are reduced to a minimum. However, as the catalyst concentration increases between 0.2% and 0.5%, the heavy components show an increasing trend. This indicates that increasing the catalyst content does not necessarily promote the catalytic oxidation reaction.
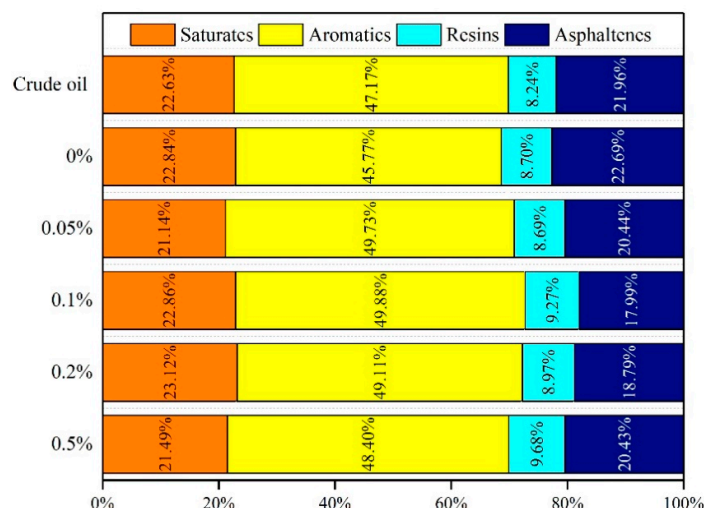
Figure 3. Effect of catalyst dosage on heavy oil group composition.

2.1.3. Effect of Amount of Oxidant

A certain amount of Tahe heavy oil, 0.1% EDDHA–FeNa catalyst, 2% THN, and different mass ratios of TBHP oxidant (0.5%, 1.0%, 1.5%, 2.0%) were added to a reactor.

As shown in Figure 4, with the increase in oxidant concentration, the light components are reduced, and the heavy components are increased. Compared with crude oil, when the oxidant concentration is 0.5%, the contents of heavy components decrease by 2.97%, with asphaltene content decreasing by 3.97%, and the upgrading effect is better. When the concentration of the oxidant continues to increase, the contents of the heavy components increase by 6.2%, 3.22%, and 5.2%, respectively, wherein the contents of asphaltene increase by 1.16%, 3.22%, and 4.16%, respectively, and the upgrading effect is slightly worse. Therefore, the optimal dosage of oxidant is 0.5%.
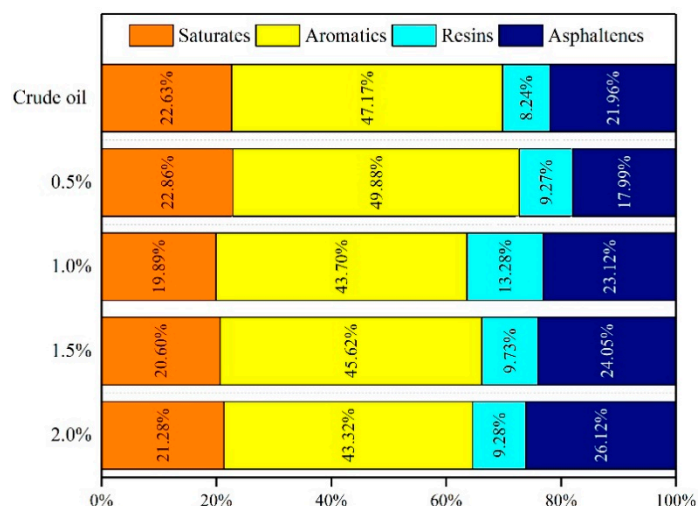

Figure 4. Effect of oxidant dosage on heavy oil group composition.

2.1.4. Effect of Reaction Temperature

As illustrated in Figure 5, the viscosity of heavy oil is inversely proportional to temperature. From 100 °C to 140 °C, the viscosity reduction effect decreases slowly, and the viscosity reduction rate only increases by 7.82%. The viscosity reduction effect is slightly worse. When the temperature reaches 140 °C, the viscosity decreases significantly. The viscosity reduction rate increases by 19.09%, and the rate of viscosity reduction reaches 82.97%. When the temperature exceeds 140 °C, although the viscosity reduction rate continues to decrease with the increase in temperature, the viscosity reduction rate increases slowly.
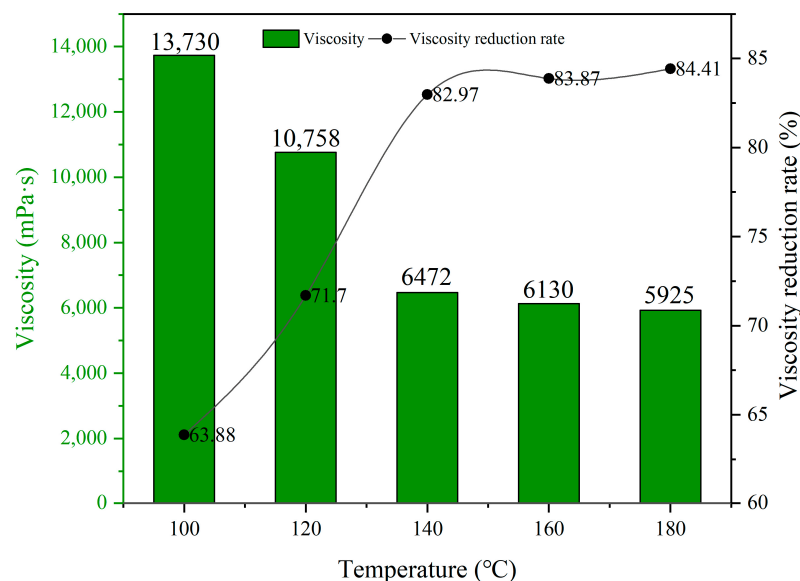
Figure 5. Effect of reaction temperature on viscosity of heavy oil.

As shown in Figure 6, when the temperature is between 100 °C and 120 °C, there is an increase in heavy components and a decrease in light components, and asphaltene content increases by 4.11% and 1.25%, respectively. It can be preliminarily concluded that during the oxidation process before 140 °C, the crude oil is mainly oxygenated. The main reaction occurs when saturated hydrocarbons and aromatic hydrocarbons in the crude oil react with the oxidant to form resins and asphaltenes, leading to an increase in heavy components. When the reaction temperature reaches 140 °C, heavy components decrease while light components increase, and asphaltene content decreases by 3.97%, 1.25%, and 0.68%, respectively. This is because, when the reaction temperature rises, the oxygen atoms added to the resin and asphaltene are released, reducing the content of resins and asphaltenes [22]. However, as the temperature continues to increase, the content of heavy components in the heavy oil rebounds to some extent. This is because the small molecular products in the pyrolysis process at low temperatures will continue to undergo a series of complex reactions such as aromatization and polycondensation to produce secondary asphaltenes and other macromolecules [23,24]. As a result, the viscosity reduction effect of crude oil is optimal at 140 °C.
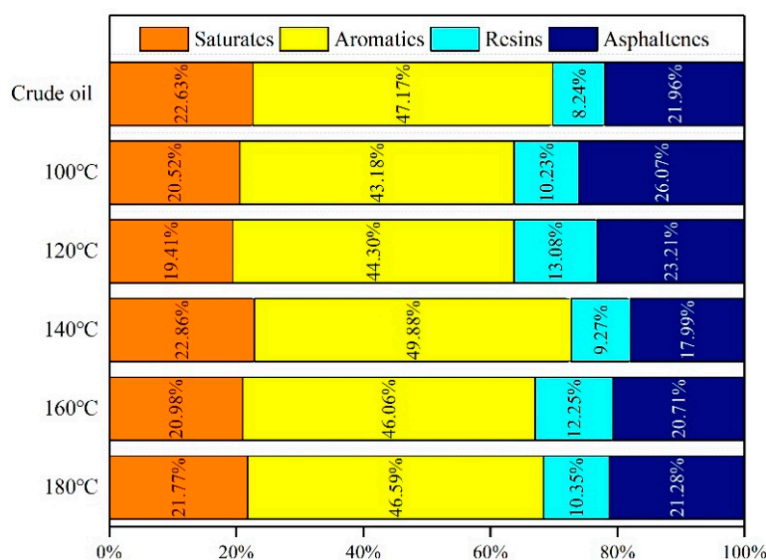

Figure 6. Effect of reaction temperature on heavy oil group composition.

2.2. Mechanism of Viscosity Reduction

2.2.1. FT–IR Analysis before and after Reaction

The FT–IR of heavy oil asphaltene before and after the reaction is shown in Figure 7a. The characteristic absorption peak of the hydroxyl group at 3448 cm^{-1} is observed. The absorption peaks at 2923 cm^{-1}, 2854 cm^{-1}, 1457 cm^{-1}, and 1375 cm^{-1} are caused by different vibrational forms of methylene and C–H bonds in methyl, respectively [25]. These peaks are strengthened at 100 °C and 120 °C, indicating that some of the light components are converted into asphaltenes. However, when the temperature exceeds 140 °C, the intensity of these peaks decreases after the reaction, indicating that the cracking reaction has occurred. The weak arch absorption peak at 1031 cm^{-1} is the characteristic peak of the S = O double bond, while the evident absorption peaks at 873 cm^{-1} and 813 cm^{-1} are characteristic peaks of polycyclic aromatic hydrocarbons and heterocyclic structures [26]. Additionally, by comparing the peak intensities, it can be observed that the peak intensities at these places are weakened, indicating that the addition of the catalyst can effectively remove the heteroatom S. The characteristic peak of the alkyl side chain of methylene ((-CH$_2$-)$_n$, $n > 4$) in asphaltene is observed at 750 cm^{-1} [27,28]. In the reaction before 140 °C, the peak intensity is enhanced, indicating the conversion of some light components into asphaltene. The drop in peak intensity after the reaction reaches 140 °C, indicates the removal of the heteroatom side chain of the polycyclic aromatic hydrocarbon.
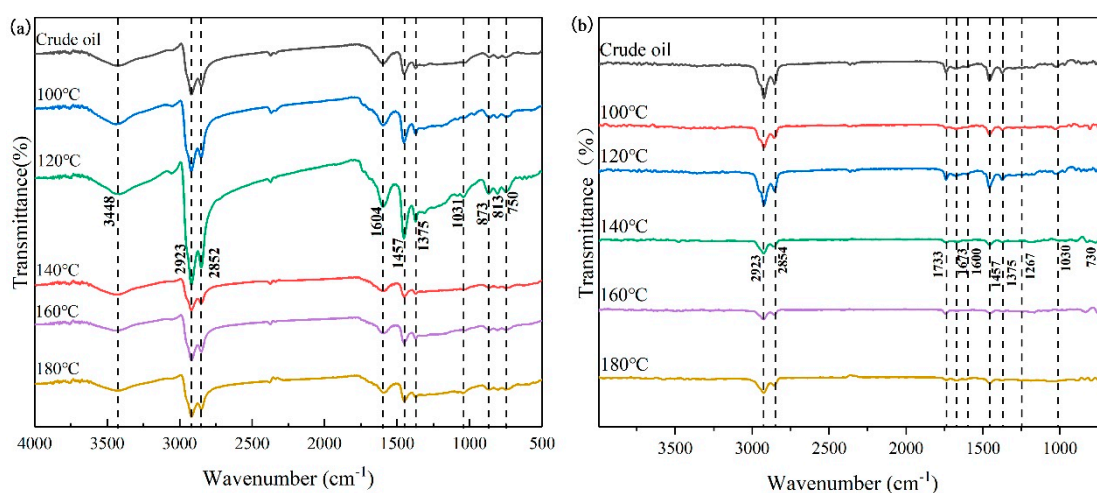

Figure 7. FT–IR spectra of asphaltene and resin before and after reaction. (**a**) Asphaltene; (**b**) resin.

The FT–IR spectra of heavy oil before and after resin reaction are shown in Figure 7b. The absorption peaks at 2923 cm^{-1}, 2854 cm^{-1}, 1457 cm^{-1}, and 1375 cm^{-1}, similar to asphaltene, are caused by different vibrational forms of C–H bonds in methylene and methyl, respectively. These peaks are enhanced at 100 °C and 120 °C. However, when the temperature exceeds 140 °C, the intensity of these peaks decreases after the reaction, indicating the occurrence of a cracking reaction. The characteristic absorption peaks of the C = O bond in ester compounds and aromatic carboxylic acid compounds are at 1733 cm^{-1} and 1673 cm^{-1}, respectively [29]. After 140 °C, the peak intensity at 1733 cm^{-1} is weakened, and the absorption peak of carboxylic acid at 1673 cm^{-1} is enhanced, indicating the oxidation of the C = O bond to COOH, and the fused ring macromolecule undergoes an oxygen addition reaction. The absorption peaks at 1030 cm^{-1} and 730 cm^{-1} belong to the S = O double bond and the side chain alkyl with a methylene number greater than four ((-CH$_2$-)$_n$, $n > 4$), respectively. The peak intensity of the two peaks drops after 140 °C, indicating the occurrence of the desulphurization reaction and the removal of the heteroatom side chain of the polycyclic aromatic hydrocarbon.

2.2.2. GC–MS Analysis before and after Reaction

The GC–MS analysis of saturates at different temperatures is presented in Figure 8. It can be observed that when the reaction temperature is below 140 °C, the peaks at C15~C19 are weaker than those of crude oil, indicating that some saturated hydrocarbons react with oxidants to form resins and asphaltenes during the oxidation process. At a reaction temperature of 140 °C, the peak intensities between C15~C19 are the strongest. As the reaction temperature increases, the peak intensities at C15~C19 become weaker. This suggests that increasing the reaction temperature promotes the conversion of heavy components into saturates through pyrolysis and the removal of alkyl side chains. Furthermore, this phenomenon elucidates that in the low temperature oxidation stage (below 140 °C), alkanes react with oxidants to produce oxygenated components, such as colloids and asphaltenes, leading to a decrease in saturated hydrocarbons.
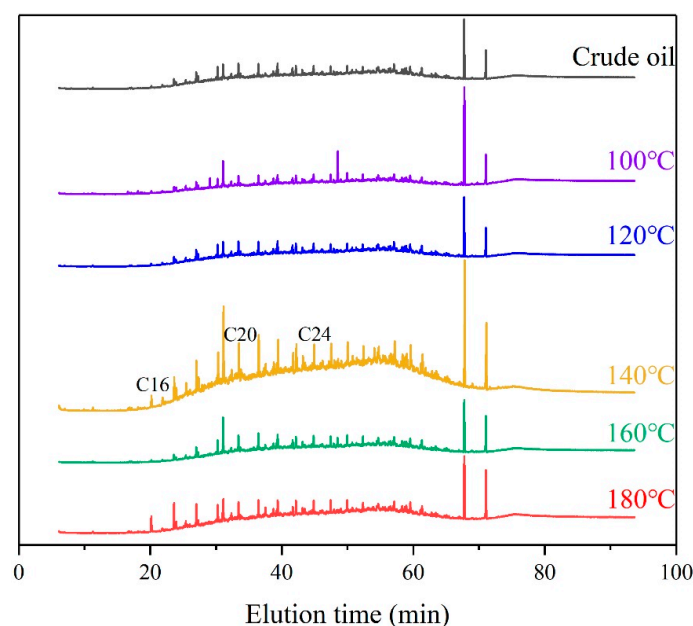

Figure 8. GC–MS analysis before and after reaction.

2.2.3. Elemental Analysis before and after Reaction

Tables 1 and 2 present the elemental analysis before and after the reaction. Resin has a higher H/C ratio than asphaltene, indicating that its ring structure or condensation degree is lower. By comparing the content of S and N in asphaltene and resin before and after the reaction, it can be found that the content of S and N in asphaltene and resin decreased at different temperatures, indicating that EDDHA–FeNa can effectively remove heteroatoms and reduce the viscosity of heavy oil. At the same time, it is evident that the removal rate of S element is much higher than that of N element, indicating that the C–S bond is more easily broken than the C–N bond [30–32].

Table 1. Asphaltene element content before and after reaction.

Samples	Element Content/%					Atomic Ratio
	C	N	S	H	O	H/C
Crude oil	83.141	1.506	4.303	6.949	4.101	1.00
100 °C	83.248	1.343	4.127	7.168	4.114	1.03
120 °C	83.352	1.331	4.114	7.306	3.897	1.05
140 °C	82.036	1.028	3.014	8.235	5.687	1.20
160 °C	83.219	1.348	4.028	7.37	4.035	1.06
180 °C	82.938	1.307	3.999	7.454	4.302	1.08

Table 2. Resin element content before and after reaction.

Samples	Element Content/%					Atomic Ratio
	C	N	S	H	O	H/C
Crude oil	81.540	1.478	4.303	9.398	4.02	1.38
100 °C	79.677	0.888	3.507	9.614	6.314	1.45
120 °C	79.488	0.878	3.287	9.531	6.816	1.44
140 °C	79.364	0.788	2.96	9.859	7.029	1.49
160 °C	79.302	0.879	3.301	9.720	6.798	1.47
180 °C	79.294	0.888	3.599	9.755	6.464	1.48

2.2.4. ^{1}H-NMR Analysis before and after Reaction

The ^{1}H-NMR results of asphaltenes and resins before and after the reaction are presented in Tables 3 and 4 and Figure 9. The aromaticity (f_A) and degree of aromatic condensation (H_{AU}/C_A) are obtained by the following formulas:

$$f_A = \frac{\frac{C_T}{H_T} - (H_\gamma + H_\beta + H_\alpha)/2H_T}{\frac{C_T}{H_T}} \tag{1}$$

$$\frac{H_{AU}}{C_A} = \frac{H_A/H_T + H_\alpha/2H_T}{\frac{C_T}{H_T} - (H_\alpha + H_\gamma + H_\beta)/2H_T} \tag{2}$$

Table 3. ^{1}H-NMR of asphaltene before and after reaction.

Samples	Components/%			
	H_γ	H_β	H_α	H_A
Crude oil	9.94	42.25	19.31	28.50
100 °C	12.72	45.43	13.19	28.66
120 °C	13.38	45.16	19.03	22.43
140 °C	12.33	43.41	19.85	24.40
160 °C	11.66	43.38	18.39	26.58
180 °C	12.09	44.07	19.20	24.64

Table 4. ^{1}H-NMR of resin before and after reaction.

Samples	Components/%			
	H_γ	H_β	H_α	H_A
Crude oil	15.72	51.57	17.65	15.07
100 °C	16.62	52.01	17.98	13.38
120 °C	16.01	54.53	18.50	10.96
140 °C	15.64	53.15	17.77	13.44
160 °C	15.65	51.74	17.63	14.98
180 °C	14.94	54.63	18.13	12.30

In Formulas (2) and (3), $\frac{C_T}{H_T}$ is the ratio of total carbon to total hydrogen, and H_T is the result of adding H_γ, H_β, H_α, and H_A. The results are shown in Tables 5 and 6.

By comparing the average molecular structure parameters of asphaltene and resin, it can be seen that the aromaticity and aromatic condensation of resin are lower than those of asphaltene. Under the actions of EDDHA–FeNa, the aromaticity of asphaltene and resin decreases at different temperatures, reaching the lowest at 140 °C, from 0.643 to 0.545 and 0.410 to 0.354, respectively, indicating that the catalyst effectively promotes the ring opening and reconstruction of aromatic rings in resins and asphaltenes. The (H_{AU}/C_A) value of asphaltene decreases from 0.594 to 0.575 and 0.568 in the reaction before 140 °C, suggesting that the condensation degree of aromatic rings increases, indicating that some

light components or alkyl side chains are re-aggregated by asphaltene components. The adsorption leads to a decrease in the condensation degree, and it also shows that the reaction before 140 °C is mainly an oxidation reaction. The (H_{AU}/C_A) value increases from 0.594 to 0.759, 0.624 and 0.619 in the reaction of asphaltene after 140 °C, which means that the condensation degree of the aromatic ring decreases. This may be caused by the ring opening of the aromatic ring and the isomerization of the side chain. However, when the temperature exceeds 140 °C, the aromatic condensation degree increases, which may be due to the fact that the small molecular products continue to undergo aromatization, polycondensation, and other complex reactions to form secondary asphaltenes.

Table 5. f_A and H_{AU}/C_A of asphaltene before and after reaction.

Samples	f_A	H_{AU}/C_A
Crude oil	0.643	0.594
100 °C	0.632	0.575
120 °C	0.592	0.568
140 °C	0.545	0.759
160 °C	0.609	0.624
180 °C	0.595	0.619

Table 6. f_A and H_{AU}/C_A of resin before and after reaction.

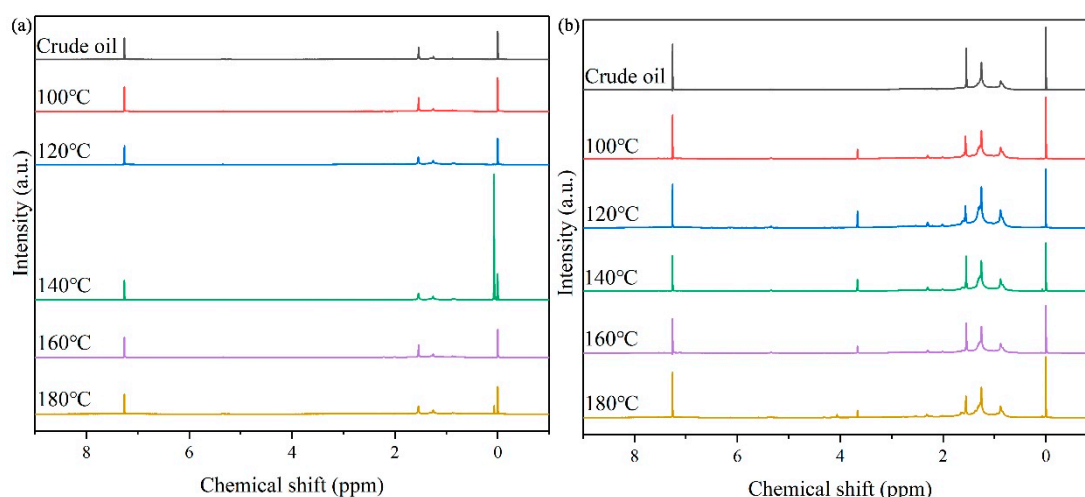| Samples	f_A	H_{AU}/C_A
Crude oil	0.410	0.809
100 °C	0.372	0.871
120 °C	0.355	0.826
140 °C	0.354	0.941
160 °C	0.375	0.933
180 °C	0.355	0.885

Figure 9. ^{1}H-NMR spectra of asphaltene and resin before and after reaction. (**a**) Asphaltene, (**b**) resin.

The aromatic condensation of resin decreases at all temperatures in comparison with the crude oil, with the lowest value occurring at 140 °C. This may be due to the isomerization of the side chain of the resin due to the addition of the catalyst. At temperatures below 140 °C, the cracking temperature required to open the aromatic ring is not reached. Thus, the oxidation reaction is still dominant. As the temperature rises above 140 °C, the closed aromatic ring opens, and the side chains are isomerized, reducing the degree of condensation of the aromatic ring.

The mechanism of catalytic oxidation viscosity reduction is analyzed through the above analysis. The oxidant can break the side chain of aromatic hydrocarbons, particularly C–S bonds. The chemical reaction equation is shown in Figure 10 [33,34].
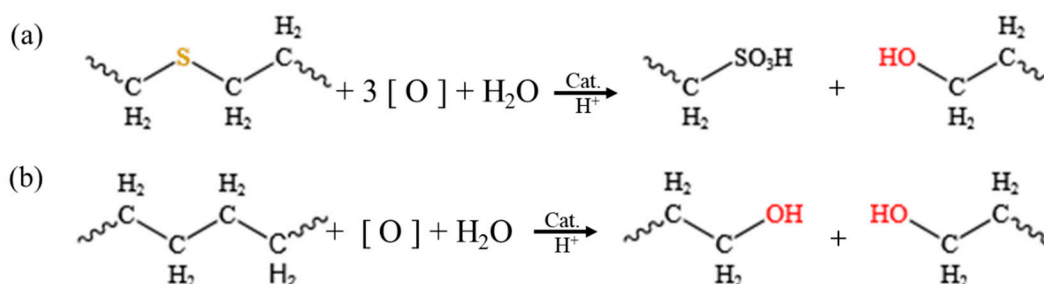

Figure 10. Mechanism of catalytic oxidation. (**a**) Mechanism of C–S bond partially connected by fused ring, (**b**) mechanism of carbon chain connected by fused ring [33,34].

3. Experiment

3.1. Materials

Commercially available chemical reagents of analytical grade were used in the experiment without any additional purification processes prior to use. Tert-butyl hydroperoxide solution (TBHP, AR, Macklin, Shanghai, China) was used as the oxidant, 1,2,3,4-tetralin (THN, AR, Macklin) was used as the proton donor, and iron naphthenate (AR, Sia reagent), ferric oleate, (AR, Macklin), EDTA–FeNa (AR, Bide Pharmatech, Shanghai, China), and EDDAH–FeNa ($C_{18}H_{16}N_2O_6FeNa$, AR, Coolaber, Beijing, China) were used as catalysts. This study used heavy oil samples from the Tahe Oilfield in Xinjiang, with a viscosity of 38,010 mPa·s at 50 °C. The group composition data are as follows: asphaltene 21.96%, resin 8.24%, saturate 22.63%, aromatic 47.17%, crude oil initial water content: 14.5%.

3.2. Low Temperature Catalytic Oxidation Experiment and Characterization

The heavy oil was first introduced into the reactor, then into the catalyst, oxidant, proton donor, and water, and the oil–water ratio was controlled at 7:3. The temperature ranged from 100 °C to 180 °C, and the reaction time was 24 h.

After the reaction, the oxidized oil was cooled to room temperature and dehydrated to determine its group composition and viscosity. The rates of the corresponding viscosity reduction were calculated. The effects of the amount of catalyst and oxidant and temperature on the properties of the heavy oil were investigated using the control variable method.

The heavy oil content before and after the reaction was determined through group composition analysis according to the 'SY/T 5119-2016 Analysis method for family compositions of rock extracts and crude oil'. The functional groups in the oxidized oil before and after the reaction were analyzed by a Fourier transform infrared detector (FT–IR, Nicolet6700, Thermo Scientific™, Waltham, MA, USA). The saturates before and after the reaction were analyzed by gas chromatography–mass spectrometry (GC–MS, 7890A/5975C). Elemental analysis of resin and asphaltene was performed using a Vario EL III automatic elemental analyzer. Deuterated chloroform was used as a solvent to dissolve resin and asphaltene for testing on an AVANCE III HD 400 MHz nuclear magnetic resonance spectrometer (1H-NMR), with trimethylsilane (TMS) serving as an internal reference. The viscosity of heavy oil before and after the reaction was measured by a Bohler Fly Rheometer DV3T-RV at 50 °C, and the viscosity reduction rate was calculated using Formula (3):

$$\Delta\eta = \frac{\eta_0 - \eta}{\eta_0} \times 100\% \tag{3}$$

where $\Delta\eta$ is the viscosity reduction rate, %, η_0 is the initial viscosity of heavy oil, mPa·s, η is the viscosity after the reaction, mPa·s.

4. Conclusions

The catalytic oxidation reaction of Tahe heavy oil has been carried out using four kinds of iron-based catalysts: iron oleate, iron naphthenate, EDTA–FeNa, and EDDHA–FeNa, in combination with the TBHP oxidant and a proton-donating acid to form a catalytic system. EDDHA–FeNa is selected as the best catalyst for catalytic oxidation among the four ferric-based catalysts, achieving a viscosity reduction rate of 78.57%. Remarkably, the metal center iron ion of EDDHA–Fe has an empty orbit and is electrophilic. These metal centers provide an empty orbit for the heteroatoms of heavy oil macromolecules, facilitating the binding of reactive oxygen species to heteroatoms and breaking the C–R (R = S, N) bond, especially the C–S bond, thereby increasing the viscosity reduction rate.

Author Contributions: Investigation, Y.M.; Data curation, L.C.; Writing—original draft, D.T.; Writing—review & editing, Z.M.; Funding acquisition, X.Y. All authors have read and agreed to the published version of the manuscript.

Data Availability Statement: The data in this article are displayed in the article.

References

1. Maity, S.K.; Ancheyta, J.; Marroquín, G. Catalytic aquathermolysis used for viscosity reduction of heavy crude oils: A review. *Energy Fuels* **2010**, *24*, 2809–2816. [CrossRef]
2. Muraza, O.; Galadima, A. Aquathermolysis of heavy oil: A review and perspective on catalyst development. *Fuel* **2015**, *157*, 219–231. [CrossRef]
3. Almao, P.P. In situ upgrading of bitumen and heavy oils via nanocatalysis. *Can. J. Chem. Eng.* **2012**, *90*, 320–329. [CrossRef]
4. Liu, Y.; Chen, E.; Wen, S. The preparation and evaluation of oil-soluble catalyst for aquathermolysis of heavy oil. *Chem. Eng. Oil Gas* **2005**, *34*, 511–512.
5. Xu, H.; Pu, C. Mechanism of underground heavy oil catalytic aquathermolysis. *Chem. Technol. Fuels Oils* **2018**, *53*, 913–921. [CrossRef]
6. Cui, Y.X.; Tang, X.D.; Meng, K.Q.; Chen, G.M.; Hu, X.Q.; Liu, D.M. Study on naphthenate and its emulsify viscosity reduction property in heavy crude oil. *Appl. Chem. Ind.* **2008**, *37*, 1409–1412.
7. Kapadia, P.; Gates, I.D.; Mahinpey, N.; Khansari, Z. *Kinetic Models for Low Temperature Oxidation Subranges Based on Reaction Products*; OnePetro: Richardson, TX, USA, 2013.
8. Zhao, J.Z.; Jia, H.; Pu, W.F.; Wang, L.-L.; Peng, H. Sensitivity studies on the oxidation behavior of crude oil in porous media. *Energy Fuels* **2012**, *26*, 6815–6823. [CrossRef]
9. Chen, Z.; Wang, L.; Duan, Q.; Zhang, L.; Ren, S. High-pressure air injection for improved oil recovery: Low-temperature oxidation models and thermal effect. *Energy Fuels* **2013**, *27*, 780–786. [CrossRef]
10. Chen, Y.; Wang, Y.; Wu, C.; Xia, F. Laboratory experiments and field tests of an amphiphilic metallic chelate for catalytic aquathermolysis of heavy oil. *Energy Fuels* **2008**, *22*, 1502–1508. [CrossRef]
11. Wang, J.; Liu, L.; Zhang, L.; Li, Z. Aquathermolysis of heavy crude oil with amphiphilic nickel and iron catalysts. *Energy Fuels* **2014**, *28*, 7440–7447. [CrossRef]
12. Galukhin, A.V.; Erokhin, A.A.; Osin, Y.N.; Nurgaliev, D.K. Catalytic aquathermolysis of heavy oil with iron tris (acetylacetonate): Changes of heavy oil composition and in situ formation of magnetic nanoparticles. *Energy Fuels* **2015**, *29*, 4768–4773. [CrossRef]
13. Al-Marshed, A.; Hart, A.; Leeke, G.; Greaves, M.; Wood, J. Optimization of heavy oil upgrading using dispersed nanoparticulate iron oxide as a catalyst. *Energy Fuels* **2015**, *29*, 6306–6316. [CrossRef]
14. Al-Marshed, A.; Hart, A.; Leeke, G.; Greaves, M.; Wood, J. Effectiveness of different transition metal dispersed catalysts for in situ heavy oil upgrading. *Ind. Eng. Chem. Res.* **2015**, *54*, 10645–10655. [CrossRef]
15. Xing, X.; Wang, X.; Pan, H.; Yuan, L.; Li, Q.; Zhang, M.; Yang, J. Fe0/graphene nanocomposite as a catalyst for the viscosity reduction of heavy crude oil. *Pet. Sci. Technol.* **2015**, *33*, 1742–1748. [CrossRef]
16. Ma, L.; Zhang, S.; Zhang, X.; Dong, S.; Yu, T.; Slaný, M.; Chen, G. Enhanced aquathermolysis of heavy oil catalysed by bentonite supported Fe (III) complex in the present of ethanol. *J. Chem. Technol. Biotechnol.* **2022**, *97*, 1128–1137. [CrossRef]
17. Liu, X.; Yang, Z.; Li, X.; Zhang, Z.; Zhao, M.; Su, C. Preparation of silica-supported nanoFe/Ni alloy and its application in viscosity reduction of heavy oil. *Micro Nano Lett.* **2015**, *10*, 167–171. [CrossRef]
18. Zhou, G.; Qin, Y.; Li, Q.; Mo, Z.; Zhang, X.; Song, L. Effect of oil displacement agent on process of low temperature catalytic oxidation of heavy oil. *J. Petrochem. Univ.* **2016**, *29*, 1.

19. Li, F.; Wang, X.; Pan, H.; Li, Q.; Yang, J. Preparation of disk-like α-Fe$_2$O$_3$ nanoparticles and their catalytic effect on extra heavy crude oil upgrading. *Fuel* **2019**, *251*, 644–650. [CrossRef]

20. Xiong, P.; Yang, H.; Wu, P.; Liao, Y.; Tan, D.; Ma, Z.; Yan, X. Study on catalytic aquathermolysis of heavy oil by simple synthesis of highly dispersed nickel-loaded nitrogen-doped carbon catalysts. *Mol. Catal.* **2022**, *529*, 112528. [CrossRef]

21. Wu, P.; Ma, Z.; Yang, H.; Xiong, P.; Tan, D.; Yan, X. Synthesis of Hierarchical Porous Fe$_2$O$_3$/Al$_2$O$_3$ Materials and Study on Catalytic Viscosity Reduction of Heavy Oil. *China Pet. Process. Petrochem. Technol.* **2022**, *24*, 98–107.

22. Yuan, C.D.; Pu, W.F.; Guo, Z.; Yao, K.L.; Liu, Z. Oxidation behavior and kinetics of light oil and heavy oil. *Chem. Eng. China* **2014**, *42*, 56–59.

23. Wang, L. Research and Application of Steam Injection to Fire Drive Mechanism for Oil Drive in Thick Oil Reservoirs. Ph.D. Thesis, China University of Petroleum (Beijing), Beijing, China, 2018.

24. Zhao, S.; Pu, W.F.; Feng, T.; Wang, W.K.; Li, Y.B. Experiments on low-temperature oxidation, pyrolysis and coking of super-heavy oil. *Spec. Oil Gas Reserv.* **2022**, *29*, 69–75.

25. Aijaz, A.; Fujiwara, N.; Xu, Q. From metal-organic framework to nitrogen-decorated nanoporous carbons: High CO$_2$ uptake and efficient catalytic oxygen reduction. *J. Am. Chem. Soc.* **2014**, *136*, 6790–6793. [CrossRef]

26. Lin, D.; Zhu, H.; Wu, Y.; Lu, T.; Liu, Y.; Chen, X.; Peng, C.; Yang, C.; Feng, X. Morphological insights into the catalytic aquathermolysis of crude oil with an easily prepared high-efficiency Fe$_3$O$_4$-containing catalyst. *Fuel* **2019**, *245*, 420–428. [CrossRef]

27. Vakhin, A.; Aliev, F.; Kudryashov, S.I.; Afanasiev, I.S. Aquathermolysis of heavy oil in reservoir conditions with the use of oil-soluble catalysts: Part II—Changes in composition of aromatic hydrocarbons. *Pet. Sci. Technol.* **2018**, *36*, 1–8. [CrossRef]

28. Avbenake, O.P.; Al-Hajri, R.S.; Jibril, B.Y. Saturates and aromatics characterization in heavy crude oil upgrading using Ni-Co/gamma-Al$_2$O$_3$ catalysts. *Pet. Sci. Technol.* **2020**, *38*, 800–807. [CrossRef]

29. Suwaid, A.M.; Varfolomeev, A.M.; Al-muntaser, A.A.; Yuan, C.; Starshinova, V.L.; Zinnatullin, A.; Vagizov, F.G.; Rakhmatullin, I.Z.; Emelianov, D.A.; Chemodanov, A.E. In-situ catalytic upgrading of heavy oil using oil-soluble transition metal-based catalysts. *Fuel* **2020**, *281*, 118753. [CrossRef]

30. Anugwom, I.; Mäki-Arvela, P.; Salmi, T.; Mikkola, J.-P. Ionic Liquid Assisted Extraction of Nitrogen and Sulphur-Containing Air Pollutants from Model Oil and Regeneration of the Spent Ionic Liquid. *Environ. Prot.* **2011**, *2*, 796–802. [CrossRef]

31. Dharaskar, S.A.; Wasewar, K.L.; Varma, M.N.; Shende, D.Z.; Tadi, K.K.; Yoo, C.K. Synthesis, characterization, and application of novel trihexyl tetradecyl phosphonium bis (2,4,4-trimethylpentyl) phosphinate for extractive desulfurization of liquid fuel. *Fuel Process. Technol.* **2014**, *123*, 1–10. [CrossRef]

32. Tang, X.D.; Chen, X.D.; Li, J.J.; Deng, L.Y.; Liang, G.J. Experimental Study on Homogeneous Catalytic Upgrading of Heavy Oil. *Pet. Chem.* **2017**, *57*, 1018–1023. [CrossRef]

33. Hayashi, J.; Aizawa, S.; Kumagai, H.; Chiba, T.; Yoshida, T.; Morooka, S. Evaluation of macromolecular structure of a brown coal by means of oxidative degradation in aqueous phase. *Energy Fuels* **1999**, *13*, 69–76. [CrossRef]

34. Hayashi, J.; Chiba, T. Quantitative description of oxidative degradation of brown coal in aqueous phase on the basis of Bethe Lattice statistics. *Energy Fuels* **1999**, *13*, 1230–1238. [CrossRef]